


Research on a physical activity tracking system based upon three-axis accelerometer for patients with leg ulcers

Rongguo Yan , Weibing Zhao, Qi Sun

School of Medical Instrument and Food Engineering, University of Shanghai for Science and Technology, Shanghai, 200093, People's Republic of China

✉ E-mail: yanrongguo@usst.edu.cn

Published in Healthcare Technology Letters; Received on 20th February 2019; Revised on 10th June 2019; Accepted on 1st July 2019

Venous leg ulcerations are a common problem, with high prevalence in the middle-aged and elderly population, and more attention on research of their physical activities has been paid, as they have great effects on the blood circulation of the lower limb. With enough, appropriate training, the chronic venous ulcerations in the lower limb can be avoided and alleviated, and venous hypertension can be reduced effectively. The study deals with a physical activity tracking system for the patients based on a three-axis accelerometer. The system uses a three-axis accelerometer, a microcontroller, and a wireless Bluetooth module to form a data acquisition platform to acquire accelerations of the lower limb movement, and sends it to a smart mobile phone via the wireless Bluetooth module. The system takes advantages of the smart mobile phone to guide the chronic venous leg ulcers to do prescribed rehabilitation exercises for the lower limb muscles, perform acceleration data preprocessing, wavelet transform and reconstruction, denoising and feature extraction, obtain the results of the rehabilitation exercises, and then give reasonable evaluation and judgment. It is helpful to treat underlying venous reflux, create such an environment that allows skin to grow across an ulcer, and accelerate ulcer healing process consequently.

1. Introduction: Chronic venous leg ulcers (CVLUs) are wounds that are thought to occur due to failure of venous return mechanisms in the lower limbs (e.g. damaged valves, past trauma from a deep vein thrombosis), which result in preventing backflow of blood and cause the pressure in veins to increase. Venous insufficiency is the most common cause of chronic leg ulceration [1–6]. In the United States, it affects ~600,000 Americans and with the prevalence increasing with age and 3.6% of people over 65 years of age are thought to be suffered from this. Annual CVLU treatment-related costs to the U.S. health care system are more than \$2 billion per year, while estimated the annual incidence of leg ulcer in the United Kingdom is about 3.5 per 1000 individuals, and treatment of venous ulcers can be expensive, leading to a large economic burden on health services, ranging between £168 and £600 million in the UK [7–9].

Patients with CVLUs experience many disabling symptoms, including pain, anxiety, depression, sleep disturbance, and itching, as well as discomfort associated with lower limb swelling, tissue inflammation, and copious wound exudate. Pain in patients with CVLUs causes significant decrements in quality of life [10–12]. Time absent from work forced early retirement, loss of functional independence and unquantifiable suffering may be another additional factor that contributes to the overall burden of CVLUs. The healing process for venous leg ulcers is typically one of the long durations, with median ulcer durations that range from six to eight months to those that last a year or even decades. Only an estimated 50–65% of CVLUs heal within six months of diagnosis, 20% remain unhealed after two years, and 8% remain unhealed after five years. Furthermore, the recurrence rate is nearly 50% [13–15].

1.1. Related work: Patients with CVLUs or more severe leg ulcers are often receiving wound care, compression therapy, or various types of wound dressings for a long period of time [16–19]. However, during ulcer treatment and care, the patients will encounter many problems using these traditional methods. For example, during wound-care, patients experience problems, such as leakage of the wound, odour, itching, pain, the timing and the time needed or available for wound care, while during

compression therapy, it is problematic due to difficulties in putting-on and taking-off elastic stockings, or bandages being painful, too tight or coming loose, warm and itching legs on hot days, also causing problems in wearing shoes [20–25].

On the one hand, since this disease occurs due to failure of venous return mechanisms in the lower limbs, it is feasible to decrease symptom associated with CVLUs and improve microcirculation and oxygen delivery by doing dedicated appropriate prescribed exercises. Such exercises may include leg elevation, pressing/pushing toes downward and upward, lifting toes upward while keeping heel firmly planted on the floor, moving forefoot like a windshield wiper, tapping forefoot up and down like keeping the beat to the music, moving forefoot like doing a figure eight etc. Although the direct effect of such exercises on healing CVLUs is unclear, its positive effect on enhancing the microcirculation in the venules, arterioles, and capillaries and hastening ulcer healing is well-documented [26, 27]. Most guidelines recommend three or four 30-min sessions of each exercise per day.

On the other hand, using accelerometer is a good way to trace such physical activity or exercise because it can provide valid and reliable measurement of its duration and intensity. The accelerometer can be worn on a variety of locations on the human body, including the wrist, hip, thigh, ankle etc. to monitor and conduct experimental studies. It has become increasingly popular due to decreased costs of the devices and a good patient-provider communication network by using a handheld smartphone. Its applications include gait & posture analysis, well-being assessment etc. [28–32].

Thus in the following Letter, we will present a lower-limb physical activity training and tracking system, which is based upon a three-axis accelerometer, for the patients with CVLUs, to guide them to do all the exercises with the aim to treat underlying venous reflux, to create such an environment that allows skin to grow across an ulcer, and to accelerate ulcer healing process consequently.

1.2. Contribution: The contribution of this Letter is twofold. First, it contributes to the healthcare field by providing the new method

that could guide the patients with leg ulcers to do the prescribed rehabilitation exercises, and accordingly treat underlying venous reflux and accelerate the ulcer-healing process. Second, it contributes to the technical field by proposing the lower-limb physical activity training and tracking system, which is based upon the three-axis accelerometer. The novelty of this method is to help the older patients to adhere to all the exercises by establishing good patient-provider communication via a handheld smartphone App. It can be implemented as a useful method to accelerate the ulcer healing process, addition to traditional wound care, compression therapy, and wound dressing.

After a general introduction to CVLUs, related work and contribution, Section 2 gives a general description of the system including the physical activity tracking device and the principle of angle conversion of the three-axis accelerometer, Section 3 demonstrates the methodology on how to perform data analysis, and Section 4 presents the results. The work's conclusions are described in Section 5.

2. Subjects and methods

2.1. Subjects: Our aim was to propose a new method to help those CVLUs to accelerate the ulcer healing process, addition to traditional wound care, compression therapy, and wound dressing. Thus, older patients aged over 55 years old, who suffered from CVLUs and were only able to walk a few feet at a time, were included during subject enrolment. However, those patients, whose symptoms were caused by arterial or diabetic ulcers, were excluded.

2.2. Foot activity tracking device: The hardware system of the foot activity tracking device is mainly composed of a microcontroller (ATmega32L), a three-axis accelerometer (ADXL335), a low-power wireless Bluetooth (B0004) based on the CC2541F256 module, a button cell (CR2032), as shown in Fig. 1a. These components are packaged in a small plastic box and the box is attached on a slipper worn by the subject using a double-sided Velcro, as shown in Fig. 1b.

When the patient performs a foot training exercise, the three-axis accelerometer can detect and analyse the linear accelerations of the foot movement in three perpendicular orientations. The low consumption microcomputer converts these analogue signals into digital ones through an analogue-to-digital (A/D) conversion, then sends data to a handheld device by using serial communication and wireless Bluetooth. The App, programmed and downloaded into the handheld device, such as iPhone, receives acceleration data, performs data processing, feature extraction, display etc. Since the App is designed for the CVLUs, the App uses one click operation, i.e. to say only one button appears in a graphical user interface (GUI) to reduce incorrect operation and help them to finish the whole training exercises by voice tips and graphical guidance.

Fig. 2a shows a picture of the device containing the three-axis accelerometer ADXL335, the microcontroller ATmega32L, and

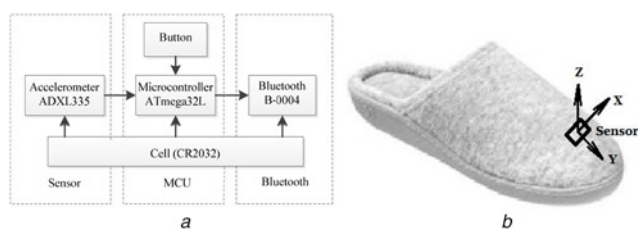


Fig. 1 Foot activity tracking device
a Main parts of the system
b Placement of the sensor



Fig. 2 Rehabilitation training system for foot exercises
a Picture of the whole device
b App and the GUI

the low-power Bluetooth B0004. Fig. 2b shows the GUI of the App on the iPhone 5C platform. The exercise shown in this figure is the heel rotation.

The main function of the iPhone-based software includes: (i) giving prompts to enter the subject's personal information; (ii) scanning and matching the possible Bluetooth device; (iii) giving help to do all the prescribed exercises; (iv) giving voice tips of the number of the week, such as, this is the second of your exercise etc.; (v) extracting the features, and uploading them to the server; (vi) promoting adherence of the subject to the prescribed physical activity and encouraging patient-provider communication, reminding the subject to do the exercise every day etc.

The subject wears a slipper with the data acquisition device on the slipper and performs foot training exercises according to the given plan to obtain the acceleration signal. Totally, there are three levels of exercises, with three exercises on each level. These nine exercises are dedicatedly designed to train the different muscles of the lower limbs to achieve a rehabilitation purpose. This study takes the heel rotation exercise as an example to illustrate how to deal with the signals.

2.3. Principle of angle conversion of three axis accelerometer: The ADXL335 is a small, thin, lower power, complete three-axis accelerometer with signal conditional voltage outputs. The three-axis acceleration sensor uses gravity as the input vector to determine the orientation of the object in the space. There are angles between the accelerometer and the horizontal direction, as shown in Fig. 3.

Assuming that the acceleration in the x -axis is A_x , the angle from A_x to the horizontal line is α_1 , and to the gravitational acceleration g is α . Similarly, the angle from A_y , which is the acceleration in the y -axis, to the horizontal line is β_1 , and to the gravitational acceleration g is β ; the angle from A_z , which is the acceleration in the z -axis, to the horizontal line is γ_1 , and to the gravitational

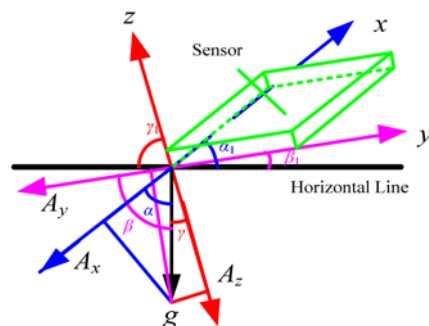


Fig. 3 Relationship between angles of three-axis accelerations and gravity

acceleration g is γ . With these angles, the following formulas can be derived [33–36]:

$$\begin{cases} \alpha = 90^\circ - \alpha_1 \\ \beta = 90^\circ - \beta_1 \\ \gamma = 90^\circ - \gamma_1 \end{cases} \quad (1)$$

The components of the gravity acceleration g in each orientation are as follows:

$$\begin{cases} A_x = g \cos \alpha = g \sin \alpha_1 \\ A_y = g \cos \beta = g \sin \beta_1 \\ A_z = g \cos \gamma = g \sin \gamma_1 \end{cases} \quad (2)$$

According to the length of a vector, it holds that $A_x^2 + A_y^2 + A_z^2 = g^2$, the relationship between the acceleration value of the three-axis accelerometer ADXL335 and the angular acceleration value (in radian) is obtained as follows:

$$\begin{cases} \tan \alpha_1 = \frac{A_x}{\sqrt{A_y^2 + A_z^2}} \\ \tan \beta_1 = \frac{A_y}{\sqrt{A_x^2 + A_z^2}} \\ \tan \gamma_1 = \frac{A_z}{\sqrt{A_x^2 + A_y^2}} \end{cases} \quad (3)$$

Then, use the data formula: $\text{radian} = \theta \pi R / 180^\circ$. This will get $\theta = \text{radian} \cdot 180^\circ / \pi$. Finally, the angle values of each axis are obtained:

$$\begin{cases} \theta_x = \frac{180}{\pi} \cdot \arctan \frac{A_x}{\sqrt{A_y^2 + A_z^2}} \\ \theta_y = \frac{180}{\pi} \cdot \arctan \frac{A_y}{\sqrt{A_x^2 + A_z^2}} \\ \theta_z = \frac{180}{\pi} \cdot \arctan \frac{A_z}{\sqrt{A_x^2 + A_y^2}} \end{cases} \quad (4)$$

Fig. 4 shows the accelerations and angles of the acceleration sensor when it is placed in a specific orientation. These values are used to verify whether the acceleration sensor is well soldered, as well as a reference for data analysis.

2.4. Data analysis: Wavelet transform, an effective multi-scale signal analysis tool, accurately reveals the distribution characteristics of the signal in time and frequency. Since it can analyse signals with multiple resolutions, it has a good application in waveform location, frequency feature extraction, and so on. In the study, we try to extract the rhythm of training signals in patients with foot ulcers by the wavelet transform. Based on the selection of wavelet basis, the optimal decomposition level, and threshold decomposition and reconstruction, the finer signals with less noises and obvious spikes are obtained. There are three steps to perform wavelet analysis as follows,

(1) Select an appropriate wavelet decomposition level and right wavelet base function to the signals with noises when performing wavelet transform, carry out wavelet decomposition to obtain the corresponding wavelet decomposition coefficients in each level, including the approximation coefficients and the detail coefficients.







No.	Orientation of the acceleration sensor	Acceleration value (g)	Angle value in each orientation (°)
1		$A_x = -1$ $A_y = 0$ $A_z = 0$	$\theta_x = -90^\circ$ $\theta_y = 0^\circ$ $\theta_z = 0^\circ$
2		$A_x = 1$ $A_y = 0$ $A_z = 0$	$\theta_x = 90^\circ$ $\theta_y = 0^\circ$ $\theta_z = 0^\circ$
3		$A_x = 0$ $A_y = 1$ $A_z = 0$	$\theta_x = 0^\circ$ $\theta_y = 90^\circ$ $\theta_z = 0^\circ$
4		$A_x = 0$ $A_y = -1$ $A_z = 0$	$\theta_x = 0^\circ$ $\theta_y = -90^\circ$ $\theta_z = 0^\circ$
5		$A_x = 0$ $A_y = 0$ $A_z = 1$	$\theta_x = 0^\circ$ $\theta_y = 0^\circ$ $\theta_z = 90^\circ$
6		$A_x = 0$ $A_y = 0$ $A_z = -1$	$\theta_x = 0^\circ$ $\theta_y = 0^\circ$ $\theta_z = -90^\circ$

Fig. 4 Output responses versus orientation gravity

(2) Select a threshold for such high-frequency coefficients. During the whole denoising process, the threshold determination is a very key point. The most suitable threshold can be selected according to the nature of the signal itself.

(3) Reconstruct the signal from its approximation coefficients and detail coefficients.

Supposed that the signal containing noise can be expressed as

$$f(t) = x(t) + m(t) \quad (5)$$

where $f(t)$ is the signal with noise from the CVLU when performing training, $x(t)$ is the real signal, and $m(t)$ is the Gaussian white noise. Then, the continuous wavelet transform of the signal $f(t)$ can be obtained as follows:

$$W_s f(t) = f(t) \varphi_s(t) = \frac{1}{s} \int_{-\infty}^{+\infty} f(\tau) \varphi\left(\frac{t-\tau}{s}\right) d\tau \quad (6)$$

where s is the scale factor, $\varphi_s(t) = (1/s)\varphi((t-\tau)/s)$ indicates expansion of wavelet bases $\phi(t)$ at level s . In the process of the actual calculation, the continuous wavelet needs to be discretised, and the most commonly used method is to carry out binary discretisation. Supposed that $S = 2^j (j \in Z)$, then, $W_2 f(t)$ is the binary wavelet transform of the signal $f(n)$.

The discrete binary wavelet transform of the sampled signal is realised by the Mallat algorithm, and the discrete signal $f(n)$ is transformed by wavelet transform; thereafter, according to different frequency channels, the multilevel decomposition is carried out. If $\varphi_{j,k}(t)$ is represented by a filter bank composed of H and L (where H is the high-pass filter, which can be expressed as, $H = \{h_j\} (j \in Z)$, and L is the low-pass filter, which can be expressed as: $G = \{g_j\} (j \in Z)$), $f(n)$ can be decomposed as follows:

$$A^{(j)}(n) = \sum_{j \in Z} g_j A^{(j-1)}(n - 2^{j-1}l) \quad (7)$$

$$D^{(j)}(n) = \sum_{j \in Z} h_j A^{(j-1)}(n - 2^{j-1}l) \quad (8)$$

where $A^{(0)}(n)$ is the discrete sample acceleration signal, $D^{(j)}(n)$ is the discrete detail signal of $f(n)(n \in Z)$ at level j , and $A^{(j)}(n)$ is the discrete approximate signal of $f(n)(n \in Z)$ at level j .

Why is wavelet transform including wavelet decomposition and reconstruction used here? As we know, during each exercise, it inevitably exists a sudden speeding up and slowing down, direction change, and jittering of the velocity. It can be considered as noise with higher frequency. The wavelet transform is used to separate signal from noise, or greatly reduce noise. It presents better characteristics than those traditional simple methods such as moving average filtering, low-pass filtering etc.

3. Results: The foot activity tracking device was fixed in a small plastic case as shown in Fig. 1b, which was attached above the patient’s slipper with the double-sided Velcro, with ADXL335 facing downward. The accelerations of three axes could be read to determine the orientations of the accelerators. Thus, when the plastic box was placed above the slipper, the initial values were listed as, $A_x = -0.19$ g, $A_y = -0.33$ g, $A_z = -0.80$ g, as shown in Fig. 5. According to the (4), the initial orientations of the accelerometer could be worked out $\theta_x = -12.4^\circ$, $\theta_y = -21.9^\circ$, and $\theta_z = -64.5^\circ$, respectively.

Fig. 5 shows accelerations along each orientation when the subject performed the heel rotation exercise. During the exercise, the subject moved the forefoot like a windshield wiper, going back and forth, keeping the entire foot on the floor with the heel not moving at slow speed about one each second. Twenty back and forth movements were in the figure. Since the forefoot moved back and forth mainly only in the x -axis direction, the fluctuation of acceleration in this direction was obviously large, as shown in Fig. 5a, while the fluctuations of accelerations in the y -axis and z -axis direction were very small, as shown in Figs. 5b and c. Therefore, we chose the acceleration in the x -axis direction as the effective recordings for later calculation.

The acceleration in the x -axis direction was re-plotted in Fig. 6a. As we know, when the subject did the heel rotation exercise, there were a sudden speeding up and slowing down, direction change, and jittering of the velocity. Rectangular boxes A and B marked in dotted line were the velocity jitters when velocity direction was suddenly changed, while C and E were the jitters in another direction, and D was the acceleration jitter during movement. These jittering values had greater impacts on calculating the frequency of the foot movement and needed to be processed first before feature extraction.

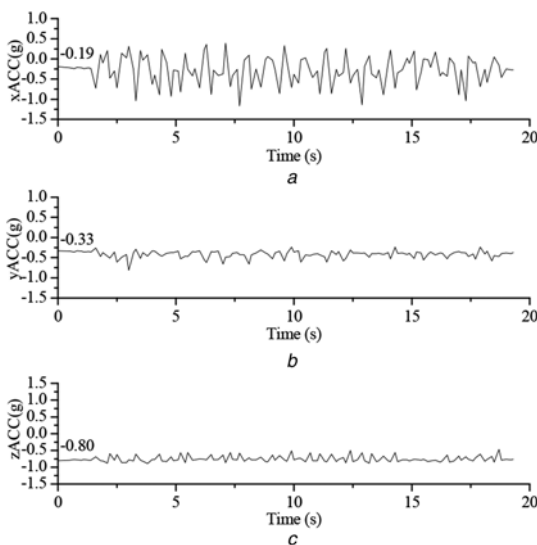


Fig. 5 Accelerations of the heel rotation exercise

Fig. 6b shows the acceleration signals after wavelet decomposition and reconstruction. The main process included:

Wavelet basis selection: the acceleration signals were processed by using Haar, db7 (Daubechies 7), db8 and db9 wavelet basis, respectively. Compared with Haar, db7 and db8 wavelet basis, db9 wavelet base with good orthogonal property could better show the periodicity of foot training. Hence, db 9 was selected in the study.

Decomposition level determination: according to the above analysis, it was most appropriate to choose the db9 wavelet base to decompose the original acceleration signal. However, if we wanted to obtain accurate training information, we needed to find the best decomposition level. With the increase of the decomposition level, the amplitude of the binary discrete wavelet was decreasing. Compared with levels 2 and 3, the acceleration waveform at level 1 remained fine, and the position of spikes could be well seen. Therefore, we selected the db9 wavelet base and the discrete wavelet decomposition for all the data [37–40].

Threshold determination: on the basis of the initial acceleration, we set a threshold for each direction of movement, called the upper threshold I and the lower threshold II, as shown in Fig. 6b. The acceleration value in the positive direction was compared with the upper threshold value I, while the acceleration value in the negative direction was compared with the lower threshold value II. The upper and lower threshold values were taken 0.03 g.

Spikes detection: in order to accurately obtain the number of foot movement or frequency, spikes detection was needed.

First, search all the potential maxima and minima in the recording waveform

$$A = X_{\max} - X_{\min} \quad (9)$$

$$P = \begin{cases} \frac{A}{K} & A > 0.025 \\ 0 & A \leq 0.025 \end{cases} \quad (10)$$

where X_{\max} and X_{\min} were a pair of adjacent local extrema of the foot ulcer training signal. From the above figure, we could see that the foot signal is quite fined, so we could use the minima and the maxima instead of its peak and valley. Here, A was the difference between the maxima and the minima. When $A \leq 0.025$, the fluctuation amplitude was very small and could be ignored

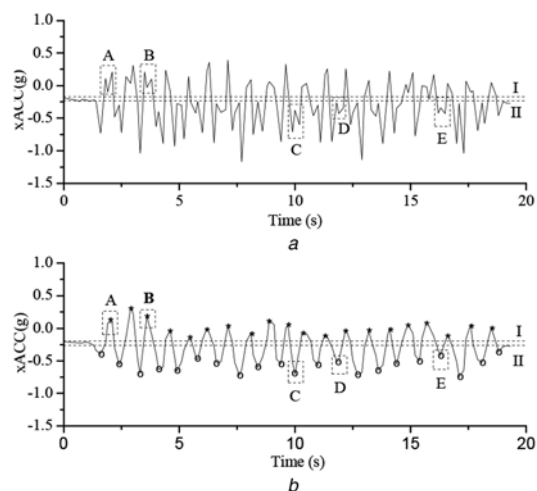


Fig. 6 Original accelerations and its wavelet reconstruction
a Original signal
b After wavelet reconstruction

Table 1 Statistical results of the heel rotation exercise of a normal subject

No.	Positive averaged training intensity, g	Negative averaged training intensity, g	Training duration, t	Training numbers	Training frequency, cpm
1	-0.01	-0.52	18	22	49
2	0.01	-0.53	18	20	54
3	0.02	-0.57	18	21	52
4	-0.02	-0.53	17	20	51
5	0.07	-0.55	16	21	46
6	0.06	-0.56	17	20	51
7	0.03	-0.52	16	20	48
8	0.17	-0.49	17	20	51
9	0.01	-0.45	16	20	48
10	0.03	-0.44	18	20	54
$\mu \pm \sigma$	0.04 ± 0.05	-0.52 ± 0.04	17.1 ± 0.88	20.4 ± 0.70	50 ± 2

(all of A, B, C and E in Fig. 6a exhibited such pseudo fluctuations). When $A > 0.025$, the fluctuation amplitude was large enough to be considered to be an effective movement. In (10), K was the maximum extrema (peak-to-peak value) and P was the training intensity that the foot ulcer gave.

According to the characteristics of accelerations, the following features were extracted [41].

- (1) *Positive averaged training intensity*. It is defined as the average value of positive acceleration peaks of the exercise in this training.
- (2) *Negative averaged training intensity*. It is defined as the average value of negative acceleration peaks of the exercise in this training.
- (3) *Duration of training*. It is defined as the time from the beginning of the exercise to the end of the exercise.
- (4) *Number of training*. It is defined as the round-trip number of exercise.
- (5) *Frequency of training*. It is measured as the number of round-trip training sessions for a given exercise per unit of time.

In the study, the heel rotation exercise was taken as an example to evaluate the correctness of the algorithm. During the exercise, the subject moved the forefoot like a windshield wiper, going back and forth from side to side, keeping the entire foot on the floor with the heel not moving at slow speed about one each second. Each training exercise from side to side had 20 reciprocating movements of the forefoot moving like a windshield wiper while keeping the heel not moving for algorithm verification purpose. The statistical results of the subject who finished ten times, each having 20 reciprocating movements are shown in Table 1.

After calculation, the positive averaged training intensity was about 0.04 ± 0.05 g, the negative averaged training intensity was about -0.52 ± 0.04 g, each training duration lasted 17.1 ± 0.88 s, the averaged training times of each exercise was about 20.4 ± 0.70 after using wavelet decomposition and reconstruction calculation, and training frequency of reciprocating movement was about 50 cycles per minute (cpm). The reason that the positive averaged training intensity approximated zero was caused by the initial position of the accelerometer. The algorithm that we used in the study reached accuracy as high as 98%.

These features will be regarded as a reference when the subject performs this exercise. If the training intensity is too low for a period of time, i.e. the amplitude or the frequency of patient's foot movement, the iPhone-based App will give appropriate voice tips to remind the patient to strengthen the amplitude and frequency of the heel rotation movement, so as to create such an environment that allows skin to grow across an ulcer and to treat underlying venous reflux.

4. Conclusion: In this study, a new wearable medical device was designed, which could help and guide the middle-aged and elderly patients to do the prescribed training exercises. The methods based upon wavelet transform, dual threshold, and spikes detection were used for signal preprocessing, processing, and feature extraction. The method based upon the wavelet transform was used to get finer waveform, dual threshold is used to eliminate the effect of smaller acceleration, while the spikes detection method is used to detect spikes, so as to know how many sessions (training numbers) there are in each exercise, and how much time each exercise performs etc. With these methods, it could quickly and effectively detect the back-and-forth number, the frequency, the duration time, and so on of each exercise.

Moreover, if the training intensity is too low for a period of time, the App will give appropriate voice tips to remind the patient to strengthen the amplitude and frequency of the exercise, so as to treat underlying venous reflux and to create such an environment that allows skin to grow across an ulcer, and to accelerate ulcer healing process consequently.

Unlike those accelerometers worn on the wrist, hip, thigh, or ankle, the accelerometer used in the study was placed above the big toe on the slipper using Velcro to monitor and conduct all experimental exercises. It could give the duration and intensity of each exercise. The main contribution lies in (i) providing a new method that could guide the patients with leg ulcers to do the prescribed rehabilitation exercises, and accordingly treat underlying venous reflux and accelerate the ulcer-healing process; (ii) proposing a lower-limb physical activity training and tracking system, which is based upon a three-axis accelerometer. By using the system, it could help the older patients to adhere to all the exercises by establishing good patient-provider communication via an App. Undoubtedly, it could be implemented as a useful method to accelerate the ulcer healing process, addition to traditional wound care, compression therapy, and wound dressing.

5. Funding and declaration of interests: The major work has been done when Rongguo Yan was in Clemson University, South Carolina, USA, as a visiting scholar, under the guidance of Associate Professor Alexey A. Vertegel from Department of Bioengineering and Professor Teresa J. Kelechi from College of Nursing, Medical University of South Carolina. The project was supported by National Institutes of Health (NIH) of USA (grant no. NCT02632695). The experiments have been carried in the Spartanburg Regional Healthcare system. The later signal processing based upon wavelet transform was carried out in the School of Medical Instrument and Food Engineering, the University of Shanghai for Science and Technology, Shanghai, China. The study has no financial or personal relationship with a third party whose interests could be positively or negatively influenced. So, on behalf of all authors, Rongguo Yan declares there is no conflict of interest.

6 References

- [1] Teresa J.K., Jan J. J., Stephanie Y.: 'Chronic venous disease and venous leg ulcers: an evidence-based update', *J. Vasc. Nurs.*, 2015, **33**, (2), pp. 36–46, doi: 10.1016/j.jvn.2015.01.003
- [2] Teresa J.K., Martina M., Dana E.K., *ET AL.*: 'Impact of daily cooling treatment on skin inflammation in patients with chronic venous disease', *J. Tissue Viability*, 2015, **24**, (2), pp. 71–79, doi: 10.1016/j.jtv.2015.01.006
- [3] Teresa J.K., Martina M., Mohan M., *ET AL.*: 'Effectiveness of cooling therapy (cryotherapy) on leg pain and self-efficacy in patients with chronic venous disease: a randomized controlled trial', *Int. J. Nurs. Stud.*, 2018, **86**, pp. 1–10, doi: 10.1016/j.ijnurstu.2018.04.015
- [4] Fedor L., Samir B., Gregory K.: 'Optimal compression therapy and wound care for venous ulcers', *Surg. Clin. North Am.*, 2018, **98**, (2), pp. 349–360, doi: 10.1016/j.suc.2017.11.006
- [5] Raffi M., O'Donnell T.F.Jr., Luis S., *ET AL.*: 'Risk factors associated with the venous leg ulcer that fails to heal after 1 year of treatment', *J. Vasc. Surg. Venous Lymphat. Disord.*, 2019, **7**, (1), pp. 98–105, doi: 10.1016/j.jvsv.2018.07.014
- [6] Behzad S.F., Shahab T., Thomas S.M., *ET AL.*: 'Prospective study of cryopreserved placental tissue wound matrix in the management of chronic venous leg ulcers', *J. Vasc. Surg. Venous Lymphat. Disord.*, 2019, **7**, (2), pp. 228–233, doi: 10.1016/j.jvsv.2018.09.016
- [7] Helen E., Kathleen F., Helen S., *ET AL.*: 'Identification of symptom clusters in patients with chronic venous leg ulcers', *J. Pain Symptom Manage.*, 2014, **47**, (5), pp. 867–875, doi: 10.1016/j.jpainsymman.2013.06.003
- [8] Matthew K.H.T., Rong L., Sarah O., *ET AL.*: 'Venous leg ulcer clinical practice guidelines: what is agreed?', *Eur. J. Vasc. Endovasc. Surg.*, 2019, **57**, (1), pp. 121–129, doi: 10.1016/j.ejvs.2018.08.043
- [9] Angela O., Una A.: 'Survey of registered nurses' selection of compression systems for the treatment of venous leg ulcers in the UK', *J. Tissue Viability*, 2019, **28**, (2), pp. 115–119, doi: 10.1016/j.jtv.2019.02.004
- [10] Elrasheid A.H.K., Khalid B., Thomas A., *ET AL.*: 'Evidence for varicose vein surgery in venous leg ulceration', *Surgeon*, 2016, **14**, (4), pp. 219–233, doi: 10.1016/j.surge.2016.03.007
- [11] Wu P., Josh P. D., Marc D. B., *ET AL.*: 'Skin perfusion responses under normal and combined loadings: comparisons between legs with venous stasis ulcers and healthy legs', *Clin. Biomech.*, 2015, **30**, (10), pp. 1218–1224, doi: 10.1016/j.clinbiomech.2015.08.001
- [12] Vesna K., Aleksandar K., Dejan P., *ET AL.*: 'Prognostic factors related to delayed healing of venous leg ulcer treated with compression therapy', *Dermatol. Sin.*, 2015, **33**, (4), pp. 206–209, doi: 10.1016/j.dsi.2015.04.005
- [13] Afsaneh A., Gary R.S., Tania J. P., *ET AL.*: 'What's new: management of venous leg ulcers: approach to venous leg ulcers', *J. Am. Acad. Dermatol.*, 2016, **74**, (4), pp. 627–640, doi: 10.1016/j.jaad.2014.10.048
- [14] Joseph D.G., Patricia M.N., Suresh V.: 'Recognition and management of venous leg ulcers', *J. Radiol. Nurs.*, 2017, **36**, (3), pp. 176–179, doi: 10.1016/j.jradnu.2017.06.002
- [15] Afsaneh A., Gary R.S., Tania J. P., *ET AL.*: 'What's new: management of venous leg ulcers: treating venous leg ulcers', *J. Am. Acad. Dermatol.*, 2016, **74**, (4), pp. 643–664, doi: 10.1016/j.jaad.2015.03.059
- [16] Jennifer A. F., Jessica K., Ian D., *ET AL.*: 'Healing of venous ulcers using compression therapy: predictions of a mathematical model', *J. Theor. Biol.*, 2015, **379**, pp. 1–9, doi: 10.1016/j.jtbi.2015.04.028
- [17] Tanja P.R., 'How to choose the proper dressing in venous leg ulcers care', *Rev. Vasc. Med.*, 2014, **2**, (2), pp. 58–61, doi: 10.1016/j.rvm.2013.12.001
- [18] Bipin K., Jinlian H., Ning P.: 'Smart medical stocking using memory polymer for chronic venous disorders', *Biomaterials*, 2016, **75**, pp. 174–181, doi: 10.1016/j.biomaterials.2015.10.032
- [19] Adam H., Arun P., Sriram R.: 'Role of compression therapy in pathophysiology of the venous system in lower limbs', *Surgeon*, 2017, **15**, (1), pp. 40–46, doi: 10.1016/j.surge.2016.08.004
- [20] Bing S., Yang W., Jacob B.: 'Gait characteristic analysis and identification based on the iPhone's accelerometer and gyrometer', *Sensors*, 2014, **14**, (9), pp. 17037–17054, doi: 10.3390/s140917037
- [21] Hugo P.: 'Compression therapy in leg ulcers', *Rev. Vasc. Med.*, 2013, **1**, (1), pp. 9–14, doi: 10.1016/j.rvm.2013.02.001
- [22] Silvia M., Alessia F., Mario S., *ET AL.*: 'Management of venous ulcers: state of the art', *Int. J. Surg.*, 2016, **33**, (s1), pp. S132–S134, doi: 10.1016/j.ijvsu.2016.06.015
- [23] Jeanne M.W.: 'Venous leg ulcers: summary of new clinical practice guidelines published August 2014 in the Journal of Vascular Surgery', *J. Vasc. Nurs.*, 2015, **33**, (2), pp. 60–67, doi: 10.1016/j.jvn.2015.01.001
- [24] Kathleen F., Min-Lin W., Helen E.E.: 'Identifying risk factors and protective factors for venous leg ulcer recurrence using a theoretical approach: a longitudinal study', *Int. J. Nurs. Stud.*, 2015, **52**, (6), pp. 1042–1051, doi: 10.1016/j.ijnurstu.2015.02.016
- [25] Una J.A., Carl T.: 'Confidence and clinical judgement in community nurses managing venous leg ulceration – a judgement analysis', *J. Tissue Viability*, 2017, **26**, (4), pp. 271–276, doi: 10.1016/j.jtv.2017.07.003
- [26] Luigi P., Cynthia K.S.: 'Medical management of venous ulcers', *Semin. Vasc. Surg.*, 2015, **28**, (1), pp. 21–28, doi: 10.1053/j.semvascsurg.2015.06.001
- [27] Phyllis G., Jeanne M.W., Melody H.: 'Venous leg ulcers: impact and dysfunction of the venous system', *J. Vasc. Nurs.*, 2015, **33**, (2), pp. 54–59, doi: 10.1016/j.jvn.2015.01.002
- [28] Sarah A. C., David R. L., Chris L., *ET AL.*: 'Associations between physical activity intensity and well-being in adolescents', *Prev. Med.*, 2019, **125**, pp. 55–61, doi: 10.1016/j.ypmed.2019.05.009
- [29] Barbara A., Patrik K., Ondrej C., *ET AL.*: 'Quantifying postural stability of patients with cerebellar disorder during quiet stance using three-axis accelerometer', *Biomed. Signal Process. Control*, 2018, **40**, pp. 378–384, doi: 10.1016/j.bspc.2017.09.025
- [30] Carly C., Anne G., Chad B., *ET AL.*: 'The impact of wearable motion sensing technology on physical activity in older adults', *Exp. Gerontol.*, 2018, **112**, pp. 9–19, doi: 10.1016/j.exger.2018.08.002
- [31] Masamitsu K., Eric J S., Tamara B H., *ET AL.*: 'Comparison of physical activity assessed using hip- and wrist-worn accelerometers', *Gait Posture*, 2016, **44**, pp. 23–28, doi: 10.1016/j.gaitpost.2015.11.005
- [32] Kingsley M.I.C., Nawaratne R., O'Halloran P.D., *ET AL.*: 'Wrist-specific accelerometry methods for estimating free-living physical activity', *J. Sci. Med. Sport*, 2019, **22**, pp. 677–683, doi: 10.1016/j.jsams.2018.12.003
- [33] Fabio A.S., Ben W.H., Claudia M.: 'Step detection and activity recognition accuracy of seven physical activity monitors', *PLOS One*, 2015, **10**, (3), p. e0118723, doi: 10.1371/journal.pone.0118723
- [34] Chih Y.Y., Jung T.H., Sheng H.T., *ET AL.*: 'A low-power monolithic three-axis accelerometer with automatically sensor offset compensated and interface circuit', *Microelectron. J.*, 2019, **86**, pp. 150–160, doi: 10.1016/j.mejo.2019.03.005
- [35] D'Emilia G., Gaspari A., Natale E.: 'Evaluation of aspects affecting measurement of three-axis accelerometers', *Measurement*, 2016, **77**, pp. 95–104, doi: 10.1016/j.measurement.2015.08.031
- [36] Yu-Sheng L., Hsuan-Wen W., Sheng-Hao L.: 'An integrated accelerometer for dynamic motion systems', *Measurement*, 2018, **125**, pp. 471–475, doi: 10.1016/j.measurement.2018.05.019
- [37] Bamberg S.J.M., Ari Y.B., Donna M.S., *ET AL.*: 'Gait analysis using a shoe-integrated wireless sensor system', *IEEE Trans. Inf. Technol. B.*, 2008, **12**, (4), pp. 413–423, doi: 10.1109/ITTB.2007.899493
- [38] Nemirko A.P., Manilo L.A.: 'Intelligent analysis of biomedical signals for personal identification and life support systems', *Proc. Comput. Sci.*, 2019, **150**, pp. 102–108
- [39] Sridhar K., Yashodhan A.: 'Trends in biomedical signal feature extraction', *Biomed. Signal Process. Control*, 2018, **43**, pp. 41–63, doi: 10.1016/j.bspc.2018.02.008
- [40] Alexander T., Andreas E., David C.Y., *ET AL.*: 'Wavelet analysis of heart rate variability: impact of wavelet selection', *Biomed. Signal Process. Control*, 2018, **40**, pp. 220–225, doi: 10.1016/j.bspc.2017.09.027
- [41] Edwards H., Courtney M., Finlayson K., *ET AL.*: 'A randomised controlled trial of a community nursing intervention: improved quality of life and healing for clients with chronic leg ulcers', *J. Clin. Nurs.*, 2009, **18**, (11), pp. 1541–1549, doi: 10.1111/j.1365-2702.2008.02648.x